J. Cell. Mol. Med. Vol 22, No 1, 2018 pp. 576-588

The expression and functional activities of smooth muscle myosin and non-muscle myosin isoforms in rat prostate

Ping Chen [a], Jing Yin [b], Yu-ming Guo [a], He Xiao [a], Xing-huan Wang [a], Michael E. DiSanto [c], Xin-hua Zhang [a] *

[a] Department of Urology, Zhongnan Hospital of Wuhan University, Wuhan, China
[b] Department of Rehabilitation, Zhongnan Hospital of Wuhan University, Wuhan, China
[c] Department of Surgery and Biomedical Sciences of Cooper Medical School of Rowan University, Camden, NJ, USA

Received: December 22, 2016; Accepted: July 10, 2017

Abstract

Benign prostatic hyperplasia (BPH) is mainly caused by increased prostatic smooth muscle (SM) tone and volume. SM myosin (SMM) and non-muscle myosin (NMM) play important roles in mediating SM tone and cell proliferation, but these molecules have been less studied in the prostate. Rat prostate and cultured primary human prostate SM and epithelial cells were utilized. *In vitro* organ bath studies were performed to explore contractility of rat prostate. SMM isoforms, including SM myosin heavy chain (MHC) isoforms (SM1/2 and SM-A/B) and myosin light chain 17 isoforms ($LC_{17a/b}$), and isoform ratios were determined *via* competitive RT-PCR. SM MHC and NM MHC isoforms (NMMHC-A, NMMHC-B and NMMHC-C) were further analysed *via* Western blotting and immunofluorescence microscopy. Prostatic SM generated significant force induced by phenylephrine with an intermediate tonicity between phasic bladder and tonic aorta type contractility. Correlating with this kind of intermediate tonicity, rat prostate mainly expressed LC_{17a} and SM1 but with relatively equal expression of SM-A/SM-B at the mRNA level. Meanwhile, isoforms of NMMHC-A, B, C were also abundantly present in rat prostate with SMM present only in the stroma, while NMMHC-A, B, C were present both in the stroma and endothelial. Additionally, the SMM selective inhibitor blebbistatin could potently relax phenylephrine pre-contracted prostate SM. In conclusion, our novel data demonstrated the expression and functional activities of SMM and NMM isoforms in the rat prostate. It is suggested that the isoforms of SMM and NMM could play important roles in BPH development and bladder outlet obstruction.

Keywords: prostate • smooth muscle • myosin • non-muscle myosin • isoforms

Introduction

Benign prostatic hyperplasia (BPH) is the most common pathologic process causing lower urinary tract symptoms (LUTS) and erectile dysfunction (ED) in ageing men with a histologic prevalence of approximately 50% for men in their 60s, and 90% for men in their 80s [1]. Although the aetiology of BPH is not well understood, androgens and ageing are necessary for the development of BPH [2] containing two physiological components: static (increased prostate size) [3] and dynamic (increased prostatic smooth muscle (SM) tone) [4]. The current standard pharmacotherapy for bothersome BPH/LUTS is α1-adrenergic antagonists (α-blockers) and antiandrogenic 5α-reductase inhibitors, targeting the dynamic and static components, respectively [2, 5]. However, 5α-reductase inhibitors are only indicated for patients with prostate volumes over 40 ml. Thus, dynamic components may play a more important role in BPH.

Indeed, pathological studies have found that the ratio of the stroma (composed mainly of SM) to the epithelium in normal human prostate is 2:1, while it is 5:1 in BPH patients [6]. We also found the SM scattered throughout the rat prostate stroma and that contraction is significant generated in response to an α1-adrenergic agonist [7]. Generally, stimulation of the adrenergic nervous system [8] can increase intracellular Ca^{2+} concentration ($[Ca^{2+}]i$) or the calcium sensitivity (when $[Ca^{2+}]i$ returned to basal levels), inducing thin filaments to slide past thick filaments (producing force) and preventing myosin dephosphorylation, which involves the RhoA/Rho-kinase (ROK) mechanism (maintaining force) [9]. Thin filaments are mainly composed of actin. Thick filaments are mainly composed of myosin, which is the motor molecule of the SM contractile apparatus. SM myosin (SMM) is composed of a pair of myosin heavy chains (MHCs) and two pairs of myosin light chains (LC_{17} and LC_{20}) that are intimately intertwined [10]. Both the 3′ and 5′ end of the MHC pre-mRNA are alternatively spliced to generate COOH-terminal isoforms (SM1 and SM2) and NH_2-terminal isoforms (SM-A and SM-B), respectively

*Correspondence to: Dr. Xin-hua ZHANG, M.D., Ph.D.
E-mail: zhangxinhuad@163.com

doi: 10.1111/jcmm.13345

[11, 12]. In addition, the essential light chain (LC_{17}) is alternatively spliced and has two 3′ end isoforms (LC_{17a} and LC_{17b}) [13, 14]. As shown in Figure 1A, the isoform-specific difference at the COOH terminus of the MHC is a length difference of 34 amino acids (AAs) (tail insert, SM1 is longer than SM2), while the isoform-specific difference at the NH_2 terminus of the MHC is 7 AAs at loop 1 (head insert, SM-A = no insert, SM-B = head insert). SMM with the head insert (SM-B) and the tail insert (SM1) is 1,979 AAs long, whereas the SM MHC without the head insert (SM-A) and the tail insert (SM2) is 1,938 AAs long. Meanwhile, $LC_{17a/b}$ isoforms have the same size (151 AAs) but differ in five of the last nine COOH AAs. The SMM isoform composition has been demonstrated to affect force development [15] as well as force maintenance [16]. The SM-B, LC_{17a} and SM2 isoforms are associated with a faster more phasic-type contraction (*e.g.* urinary bladder), whereas the SM-A, LC_{17b} and SM1 isoforms are associated with a slower more tonic force generation (*e.g.* aorta) [17–21]. We have demonstrated that the corpus cavernosum (CC) SM possesses a myosin isoform composition somewhat intermediate between bladder and aortic SM, considered to exhibit phasic and tonic characteristics, respectively [22]. With regard to the prostate, no study has thoroughly characterized its SMM isoforms and correlating contractility profiles.

Similar to SMM, non-muscle myosin (NMM) molecules are comprised of three pairs of peptides: two heavy chains, two regulatory light chains that regulate NMM activity and two essential light chains that stabilize the heavy chain structure. The NM MHC isoforms in mammalian cells result from three different genes (MYH9, MYH10 and MYH14) encoding NM MHC proteins (NMMHC-A, NMMHC-B and NMMHC-C, respectively) [23–26]. As shown in a schematic figure (Fig. 1B), the NMMHC-A and NMMHC-B isoforms are more similar in size (NMMHC-A is 1,960 AAs long and NMMHC-B is 1,976 AAs long) to the SM MHC isoforms than NMMHC-C (1,995 AAs). Indeed, the NMMHC-C isoform has an additional 20 AAs at the NH_2 terminus and shows significantly more variability in AA sequence than NMMHC-A and NMMHC-B [27]. Although these myosin isoforms are referred as 'non-muscle' myosin IIs to distinguish them from their muscle counterparts, they are also present in muscle cells, where they have distinct functions during skeletal muscle development and differentiation [28], as well as in the maintenance of tension of SM [29, 30]. In addition, NMM is central in the control of cell migration and cytokinesis and tissue architecture owing to its position downstream of convergent signalling pathways [31–34]. A previous study found NMM expressed higher in embryonic or newborn tissues when compared to adult tissues [35], and the relative percentage of the NMM decreased significantly as the animals reached maturity [36]. Thus, NMM might be known as embryonic myosin. Actually, NMM isoforms are expressed in a spatiotemporal manner during embryogenesis and adulthood. We also previously found that expression of NMMHC-B was greatly increased by 4.5-fold in bladder of partial bladder outlet obstruction rat model [37]. Thus, NMM might be interacting with the

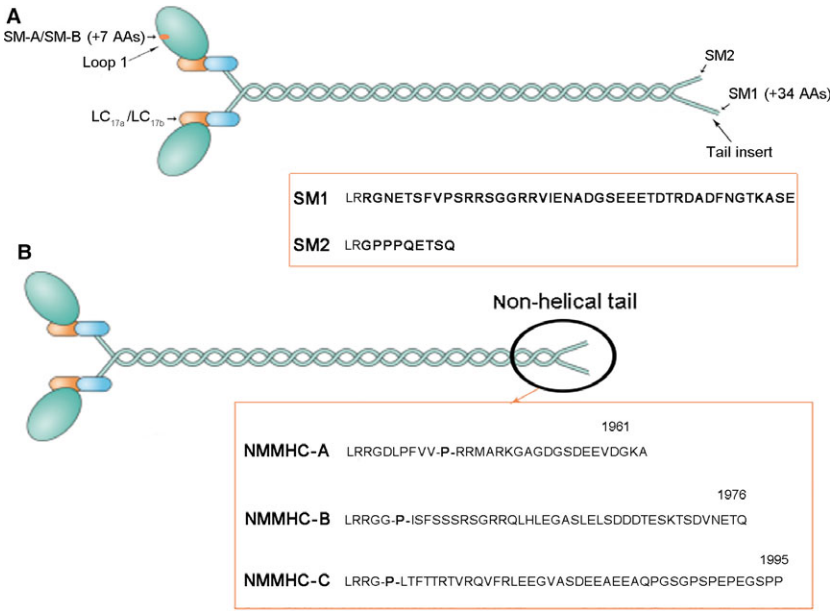

Fig. 1 The schematic figure of isoform-specific differences between the SMM, NMM and LC_{17} isoforms. (A) The isoform-specific differences of SMM. The SM MHC subunits derive from two alternative splices, one is a length difference of 34 amino acids (AAs) (a sequence difference of 43 AAs) at the non-helical COOH terminus of the MHC (tail insert; SM1 is the longer tail and SM2 is the shorter tail) and the other one is the addition of 7 AAs at loop 1 (head insert; SM-A = no insert, SM-B = head insert). In addition, (A) shows that while $LC_{17a/b}$ isoforms are the same size (151 AAs), they differ in 5 of the last 9 COOH AAs. (B) The isoform-specific differences of NMM. The NMMHC-A and NMMHC-B isoforms are similar in size (NMMHC-A is 1,960 AAs long and NMMHC-B is 1,976 AAs long). The NMMHC-C isoform has an additional 20 AAs at the NH_2 terminus (1,995 AAs). Sign '-P-' means beginning non-helical tail.

Journal of Cellular and Molecular Medicine published by John Wiley & Sons Ltd and Foundation for Cellular and Molecular Medicine.

pathophysiological process of some diseases. BPH has been suggested to be a 'reawakening' of embryonic processes in which embryonic prostatic mesenchyme dictates differentiation of new epithelial gland formation, which is normally seen only in foetal development [38–42]. Therefore, NMM may indeed play important roles in BPH development.

At the functional level, blebbistatin (BLEB), a small cell permeable selective myosin II inhibitor, was originally discovered as the result of a high-throughput screen for inhibitors of NMM [16]. More recently, BLEB has been suggested to inhibit SM contraction with near equipotency as for NMM [43–45]. Eddinger *et al.* [43] showed that force maintenance of chicken carotid artery was inhibited by BLEB (IC_{50}, 3 μM). Also, our previous studies showed BLEB could inhibit the force maintenance of rat and human CC and bladder [44, 45]. However, BLEB efficacy on prostate tension remains to be elucidated.

The aim of the current study was to determine SMM and NMM expression and isoform composition in the prostate, as well as their functional activities.

Materials and methods

Chemicals and tissues

All chemicals were purchased from Sigma-Aldrich (St. Louis, MO, USA) except (±) BLEB and H-1152 were from Tocris (Ellisville, MO, USA). The racemic mixture (±) of BLEB was used in all studies as it was determined that the active (−) enantiomer form was equipotent to the (±) racemic mixture in the *in vitro* studies and that the inactive (+) form did not induce significant relaxation [16, 43, 44, 46]. A stock solution of (±) BLEB was made in dimethylsulphoxide (DMSO); the other substances were dissolved daily in double distilled water. Control experiments showed that the final concentration of 1/1000 (V/V) DMSO used in these studies did not significantly modify the relaxation response. Due to the known light sensitivity of BLEB, it was always kept in the dark in the refrigerator until just prior to usage and during the experiment, the organ bath chambers were kept covered. Male rat prostate, urinary bladder, CC and aorta were obtained from 10 Sprague Dawley rats weighing 300–350 g (Animal Center of Zhongnan Hospital of Wuhan University). All animal studies were approved by the research committee of Zhongnan Hospital of Wuhan University. Human prostatic smooth muscle cells (HPrSMCs) and epithelial cells (HPrECs) were purchased from Lonza (Walkersville, MD, USA). All strips including all three dimensions of approximately 1 cm were prepared for organ bath physiology studies and immediately placed in Krebs-Henseleit (Krebs) solution with the rest of the tissue frozen in liquid nitrogen and saved at −80°C for subsequent molecular analyses or placed into 10% neutral buffered formalin for histological examination. All surgical procedures were performed under anaesthesia by intraperitoneal injection of sodium pentobarbital (35 mg/kg; Abbott Laboratory; Chicago, IL, USA).

In vitro organ bath studies

As previously described [45, 47], rat prostate, bladder detrusor, CC and aorta strips were mounted longitudinally in a 4 ml organ bath—Multi-Myograph Model 810MS (Danish Myo Technology; Aarhus, Denmark). The myograph was connected in line to a PowerLab 4/30 Data Acquisition System (ADInstruments; Colorado Springs, CO, USA) and in turn to a Dual-Core processor Pentium computer for real-time monitoring of physiological force. The SM strips were equilibrated at least 1 hr in Krebs buffer [45, 47] at 37°C with continuous bubbling of 95% O_2 and 5% CO_2. The buffer had the following mM composition: NaCl 110, KCl 4.8, $CaCl_2$ 2.5, $MgSO_4$ 1.2, KH_2PO_4 1.2, $NaHCO_3$ 25 and dextrose 11, and it was changed every 15 min. Strips were continuously adjusted to resting tension (0.5 g for rat prostate, 1.5 g for rat bladder, 0.35 g for rat CC and 0.7 g for rat aorta) [48–51]. After equilibration, the tissues were contracted with 60 mM KCl. This degree of contractile response was taken as 100% and the force induced by different concentrations of the various agonists (phenylephrine (PE) for prostate, CC, aorta and carbachol for bladder) was expressed as a percentage of this value. After washing several times to baseline with Krebs buffer, prostate strips pre-contracted with 1 μM PE at a concentration pre-determined to produce submaximal force were allowed to reach stable tension, and then, the relaxant effect of increasing doses of BLEB (1, 5, 10 μM), nitric oxide (NO) donor sodium nitroprusside (SNP) (10^{-8}–10^{-4} M) and the Rho-kinase inhibitor (H-1152) (10^{-9}–10^{-5} M) was evaluated.

RNA extraction and cDNA synthesis

Total RNA was extracted using TRIzol reagent (Invitrogen, Carlsbad, CA, USA) according to the manufacturer's protocol. Briefly, the tissue was ground into a powder using a mortar and pestle cooled in liquid nitrogen, without allowing the tissue to thaw. The powder then was homogenized immediately in denaturing buffer using a T8 Ultra-Turrax minielectric homogenizer (IKA Works; Wilmington, NC, USA), chloroform was added and mixed, the phases separated by centrifugation, and the RNA precipitated by isopropanol and then washed with 75% ethanol and dissolved in RNase-free sterile water. The resulting RNA was quantitated by spectrophotometry at 260/280 nm. Total RNA (1 μg) then was reverse transcribed using 0.5 μg oligo $(dT)_{12–18}$ primer, 500 μM dNTPs (Invitrogen) and 200 U of SuperScript II RNase H reverse transcriptase in a total volume of 20 μl for 50 min. at 42°C.

Competitive reverse transcriptase polymerase chain reaction (competitive RT-PCR)

As previously reported [20, 37], differences of nucleic acid sequence in each pair of SMM isoforms were quite small, so competitive RT-PCR was applied to detect the expression of SMM isoforms. Polymerase chain reaction (PCR) was performed on 100 ng of the reverse transcribed cDNA using 2 units of Red Taq DNA polymerase (Sigma-Aldrich), 200 ng each of upstream and downstream primer and 200 μM dNTPs (Invitrogen). SM-A/SM-B, SM1/SM2 and LC_{17a}/LC_{17b} alternatively splice isoforms were amplified with competitive PCR, using a GeneAmp 9700 thermal cycler (Applied Biosystems, Foster City, CA, USA). The primer sequences are shown in Table 1. The cycling conditions were an initial 5 min. at 94°C followed by 35 cycles (30 sec. at 94°C, 30 sec. at 55°C and 120 sec. at 72°C), ended by a final one-time 7-min. incubation at 72°C to ensure extension of all products. The fact that all three pairs of myosin isoforms are generated *via* alterative splicing allowed us the opportunity to perform competitive PCR for each primer pair by designing primers that flanked the insert region.

The PCR products were then separated by electrophoresis on a 2.5% agarose gel and were visualized using GelStar staining and ultraviolet illumination. Band density was quantified by reflectance scanning of gel photographs obtained with a BioDoc-It camera set-up (UVP; Upland, CA, USA) using a Bio-Rad (Hercules, CA, USA) GS-700 imaging densitometer and subsequent analyses using the Bio-Rad Molecular Analyst 1D program that enabled us to obtain quantitative relative SMM isoform expression data for all isoform pairs.

Real-Time reverse transcriptase polymerase chain reaction (Real-Time RT-PCR)

As previously reported [37], RT products were also amplified in a 96-well plate in a 25 μl reaction volume with all samples run in triplicate, using the model 7300 Real-Time Thermocycler (Applied Biosystems). The following experimental protocol was utilized: denaturation (95°C for 10 min. to activate the polymerase) followed by an amplification programme repeated for 40 cycles (95°C for 15 sec., then 60°C for 60 sec.) using a single fluorescence measurement. SM MHC- and NM MHC-targeted genes were amplified using SYBR Green for amplicon detection. For relative quantification, the efficiency of amplification for each individual primer pair (sequences shown in Table 1) was determined using cDNA target and the $2^{-\Delta\Delta ct}$ method [52] in conjunction with the RQ Study Software version 1.2.3 (Applied Biosystems). Gene expression was normalized to expression of the RPL19 ribosomal housekeeping gene as an internal control.

SDS-PAGE and Western blotting analysis

As previously described [47], proteins were extracted from frozen tissue samples using the CelLyticTM NuCLEARTM Extraction kit (amsbio; Abingdon, UK) and 30 μg of each sample was electrophoresed on a 10% SDS-polyacrylamide gel and transferred to nitrocellulose membrane (Amersham Pharmacia; Piscataway, NJ, USA) by semidry electroblotting for 1 hr. The membrane was blocked for 2 hr at room temperature with 5% non-fat dried milk dissolved in phosphate-buffered saline (PBS) solution. The membranes were incubated overnight at 4°C with primary SM MHC (1:200, Santa Cruz, mouse monoclonal to MYH11, sc-6956), NMMHC-A (1:1000, Abcam, rabbit polyclonal to non-muscle Myosin IIA, ab75590), NMMHC-B (1:2000, Abcam, rabbit polyclonal to non-muscle Myosin IIB, ab204358) and NMMHC-C antibody (1:200, Santa Cruz, goat polyclonal to MYH14, sc-138037). After washing several times with PBS, the membranes were incubated with anti-mouse or anti-rabbit or anti-goat immunoglobulin G (IgG) linked with horseradish peroxidase at a 1:10,000 dilution (Thermo Scientific Fisher; Rockford, IL, USA) for 1 hr at room temperature. Detection of reaction antigen was performed with an enhanced chemiluminescence (ECL) kit (Thermo Scientific Fisher). A monoclonal mouse antibody against GAPDH (1:5000; Sigma-Aldrich) was used as a control to ascertain equivalent loading.

Immunohistochemistry

Tissues fixed in 10% neutral buffered formalin for 24–36 hrs were routinely processed for paraffin embedding. Samples for immunohistochemistry (IHC) were sectioned at 5 μm and deparaffinized in xylene followed by descending grades of alcohols (100%, 95%, 70%, 30%). Antigen retrieval was performed in 10 mM sodium citrate buffer at pH 6.0, heated to 96°C, for 30 min., followed by proteinase K treatment for 10 min. Endogenous peroxidase activity was quenched using 3% hydrogen peroxide in PBS for 15 min. Blocking was performed by incubating sections in 5% normal donkey serum with 2% BSA for 1 hr. The sections were stained by routine IHC methods, using horse radish peroxidase polymer conjugate (Invitrogen), to localize the antibody bound to

Table 1 Primer sequences used to amplify target genes by PCR

Target gene	Primer	Primer sequence
SM-A/-B	Forward	5′-GGCCTCTTCTGCGTGGTGGTC-3′
	Reverse	5′-TTTGCCGAATCGTGAGGAGTTGTC-3′
$LC_{17a/b}$	Forward	5′-GAGAGTGGCCAAGAACAA-3′
	Reverse	5′-CAGCCATTCAGCACCATGCG-3′
SM1/2	Forward	5′-GCTGGAAGAGGCCGAGGAGGAATC-3′
	Reverse	5′-GAACCATCTGTGTTTTCAATAA-3′
SM MHC	Forward	5′-TTTGCCATTGAGGCCTTAGG-3′
	Reverse	5′-GTTCACACGGCTGAGAATCCA-3′
NM MHC (MYH10)	Forward	5′-TGAGAAGCCGCCACACATC-3′
	Reverse	5′-CACCCGTGCAAAGAATCGA-3′
RPL19	Forward	5′-GCGTCCTCCGCTGTGGTA-3′
	Reverse	5′-CATTGGCGATTTCGTTGGT-3′

MHC: myosin heavy chain; NM: non-muscle; SM: smooth muscle; LC: light chain; RPL19: ribosomal protein L19.

Journal of Cellular and Molecular Medicine published by John Wiley & Sons Ltd and Foundation for Cellular and Molecular Medicine.

antigen, with diaminobenzidine as the final chromogen. All immunostained sections were lightly counterstained with haematoxylin. The primary antibody to myosin heavy chain (SM MHC) (1:100) was incubated for 1 hr at room temperature. Primary species (mouse IgG) was substituted for the primary antibody to serve as a negative control. Slides were evaluated for immunostaining by light microscopy.

Confocal microscopy

HPrSMCs and HPrECs were resuspended in nutrient medium containing 10% foetal calf serum and a high concentration (15 mM) of thymidine to prevent cell division. Glass coverslips were coated with collagen (a drop of 1 mg/ml rat tail collagen in 5% acetic acid; Sigma Chemicals) and kept in 60-mm tissue culture dishes overnight under UV light to polymerize the collagen. These dishes were rinsed with balanced salt solution to remove the acid, and the cells were plated in the culture dishes and fed with nutrient medium containing 10% foetal calf serum and 15 mM thymidine and incubated overnight. The next day, cells were attached on the collagen substratum coated on the coverslip. These cultures were fixed in 5% buffered formalin, kept in the refrigerator for 4 hr and processed for confocal microscopy.

Fixed cells were washed three times with PBS for 2 min. each time and incubated in blocking solution (1% BSA in PBS) for 30 min. Cells and rat prostate sections were then incubated for 1 hr at room temperature with the previously employed antibodies against NMMHC-A (1:200), NMMHC-B (1:100) or NMMHC-C (1:50). The slides were then washed three times with PBS and reacted with anti-rabbit or anti-goat IgG made in goat labelled with TRITC. The slides were then washed three times in PBS and reacted with antibody specific to the whole SM MHC (1:100) labelled with FITC-antimouse. Slides were washed three times in PBS, stained with DAPI for 3 min. to label nuclei and mounted in Vectashield mounting medium (Vector Laboratories; Burlingame, CA, USA), and the fluorescence signal was detected using confocal laser scanning microscopy (Carl Zeiss LSM 510, Carl Zeiss; Jena, Germany). Negative controls were prepared by replacing the primary antibody with preimmune serum.

Statistical analysis

Results are expressed as mean ± S.E.M. for n experiments. Statistical analysis used either the Student's t-test with Excel software (two sample treatments compared) or ANOVA and Bonferroni post-tests with GraphPad Prism 5.0 (multiple means compared). $P < 0.05$ was considered significant.

Results

The prostate is mainly composed of stroma (SM cell) and epithelium. Figure 2A and B are cultured human prostate SM and epithelium cells, respectively. As shown in Figure 2C and D, immunohistology and immunofluorescence demonstrated that prostatic SMM immunolocalized with the SM-specific marker MHC was abundantly displayed in the rat prostate, predominantly in the outer stromal layer (black arrows). Thus, we investigated the contractility of prostate *in vitro*. Prostatic SM per se generated significant force in response to KCl depolarization and PE-mediated adrenergic stimulation in a dose-dependent manner. Figure 3A is representative tracing of rat prostate SM contraction in response to KCl and PE. The PE dose–response contractions were normalized to KCl-elicited force and were averaged in Figure 3B. Isolated prostatic strips from rats produced 17 mg force/mg tissue tension at 60 mM KCl and reached maximal contraction at the concentration of 10^{-5} M of PE. At 1 μM, the prostate strip almost reached maximum contraction and this submaximal contraction was chosen for later experiments. Figure 4A showed rat prostate exhibits intermediate tonic and phasic contractile characteristics. This tonicity was further compared with rat CC (Fig. 4B), urinary bladder (Fig. 4C) and aorta (Fig. 4D). Consistent with previous reports, bladder and aorta produced typical phasic and tonic contractility, respectively. Similar to CC, prostate SM showed tonicity between bladder and aorta.

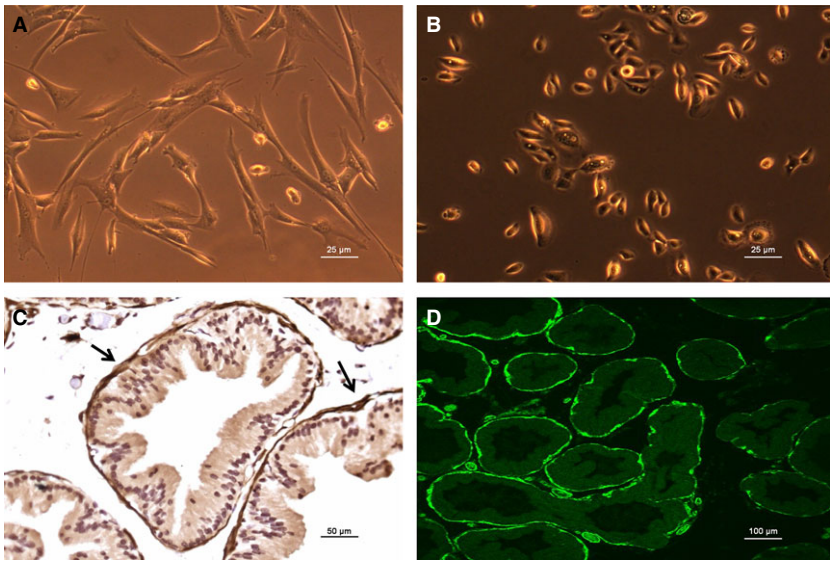

Fig. 2 Morphology of human prostatic smooth muscle cells (HPrSMCs) and epithelial cells (HPrECs) and immunolocalization of smooth muscle (SM) myosin heavy chain (MHC) in ventral prostate. (**A**) and (**B**) display morphology under the light microscope of HPrSMCs and HPrECs, respectively. (**C**) and (**D**) display immunohistology and immunofluorescence of SM MHC in the rat prostate, respectively. The black arrows show SM in the outer stroma layer of rat prostate.

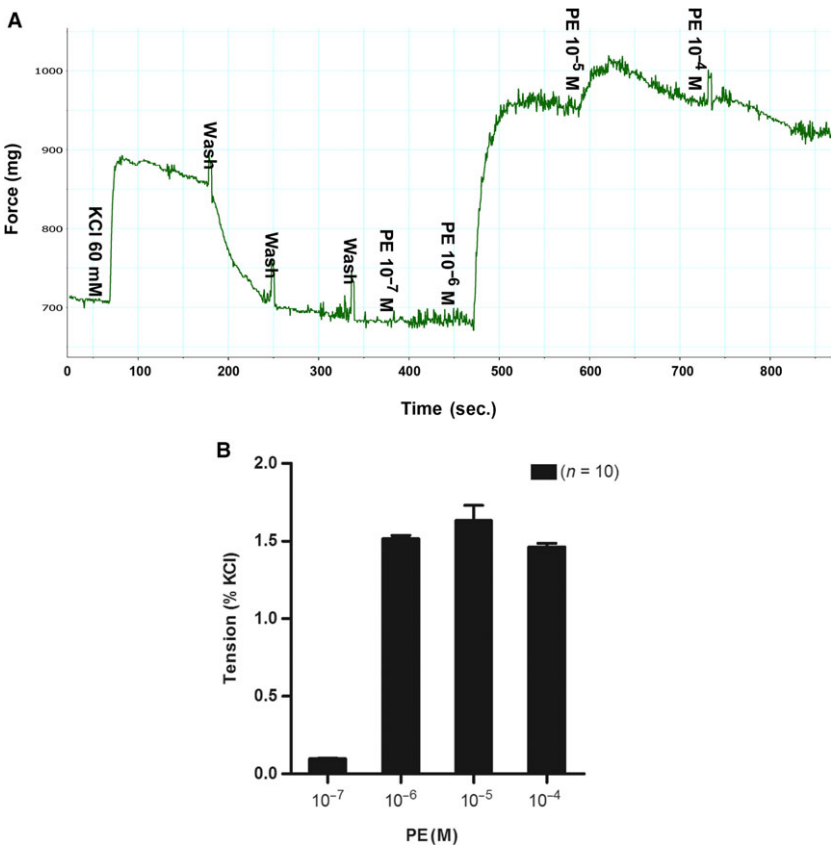

Fig. 3 (**A**) The tracing of KCl induced contraction followed by phenylephrine (PE) induced dose–response contraction for rat ventral prostate. The *x*-axis represents time (sec.), while the *y*-axis represents force (mg). (**B**) Summary graph for *in vitro* contractility of rat ventral prostate smooth muscle (SM). The maximum response to 60 mM KCl was taken as 100%, while the contractile effect of cumulative concentrations (0.1–100 μM) of PE was evaluated as a percentage of this response. Values are expressed as the mean ± S.E.M. (*n* = strips obtained from 10 different animals).

Subsequently, the compositions of SMM isoforms in the prostate, CC, bladder and aorta were examined with competitive RT-PCR. In the current study, the SM-A/B isoforms appeared to have a much wider range of expression levels than SM1/2 and $LC_{17a/b}$ isoforms. As the relative ratios of SM-B to SM-A, LC_{17a} to LC_{17b} and SM2 to SM1 were associated with contraction characteristics, we focused upon determining the percentages of SM-B, LC_{17a}, SM2 in different tissues and found they were similar to each other in the same type of samples. As demonstrated in Figure 5A and B, rat aorta expressed exclusively SM-A, less LC_{17a} and less SM2 favouring a slow tonic contraction (Fig. 4D). And rat bladder expressed 88.5% SM-B, 70.1% LC_{17a} and 30.2% SM2 exhibiting a fast phasic contraction (Fig. 4C). Rat prostate contained almost similar SM-B (58.8%), more LC_{17a} (83.8%) and less SM2 (11.4%) compared to their alternatively spliced counterparts. Similar to our previous report, rat CC contained more SM-B (70.4%), almost equal LC_{17a} (48.7%) and less SM2 (28.9%). Interestingly, both prostate and CC SMM isoform compositions favoured an intermediate tonicity profile. Also correlated with SMM isoforms, time to 50% PE-mediated maximum contraction for bladder, CC, prostate and aorta was 5.7 ± 1.2 S, 12.7 ± 2.5 S, 13.2 ± 2.6 S and 24.2 ± 2.4 S, respectively (Table 2).

We further investigated the efficacy of BLEB, a selective myosin II inhibitor, to relax rat prostate SM. As demonstrated in Figure 6A and B, BLEB strongly and dose-dependently relaxed rat prostate strips. At 3 μM, BLEB almost completely attenuated the PE pre-contracted prostatic strips. BLEB actually was capable of decreasing the tension lower than the baseline suggesting that BLEB could be useful for lowering basal prostate tone. In addition, both SNP and H-1152 also strongly and dose-dependently relaxed PE pre-contracted rat prostate (Fig. 7).

Real-Time PCR was performed to quantify the relative expression of SMM (containing SM1/2 and SM-A/B) and NMMHC-B in rat prostate and bladder. As demonstrated in Figure 8, NMMHC-B expression in rat prostate was more than 2-fold higher than that of rat bladder, while SMM expression was found to be similar.

In addition to SMM, NMM isoforms were also determined in the prostate. We used cultured HPrSMCs and HPrECs to accurately localize the SM MHC and NM MHC expression in human prostate cells. Immunofluorescence showed SMM was abundantly present only in HPrSMCs (Fig. 9A–C). NMMHC-A and NMMHC-B were both present in HPrSMCs and HPrECs (Fig. 9A and B), while NMMHC-C was found only in HPrSMCs and no expression in HPrECs (Fig. 9C). As demonstrated in Figure 9D, all NMM isoforms (NMMHC-A, B, C) were abundantly detected in rat prostate with Western blotting analysis. To accurately localize the SM MHC and NM MHC expression in rat prostate, we did immunofluorescence studies of rat prostate and found that all NMM isoforms (NMMHC-A, B, C) were abundantly detected in the stroma and epithelium of rat prostate and SM MHC was located in the stromal layer (SM cells) (Fig. 10).

Journal of Cellular and Molecular Medicine published by John Wiley & Sons Ltd and Foundation for Cellular and Molecular Medicine.

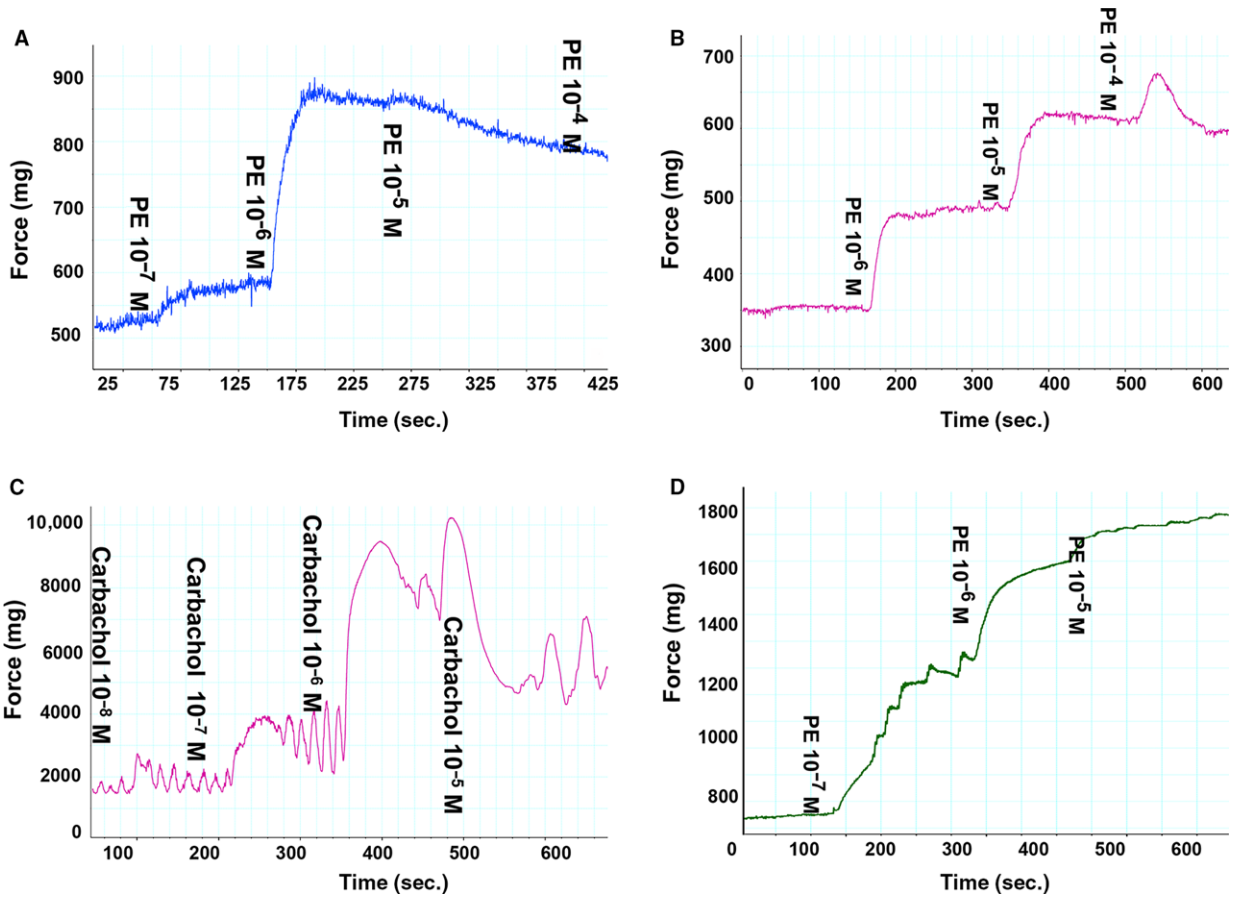

Fig. 4 *In vitro* contractility of rat ventral prostate, corpus cavernosum (CC), bladder and aorta. (**A**–**D**) Curves of phenylephrine [for prostate (**A**), CC (**B**)] and aorta (**C**)) or carbachol [for bladder (**D**)] induced dose–response contraction. The *x*-axis represents time (s), while the *y*-axis represents force (mg).

Discussion

Our novel data demonstrated the expression of isoforms of SMM and NMM and their functional activities in the prostate. Rat prostate mainly expressed LC_{17a} and SM1 but with relatively equal expression of SM-B at the mRNA level, correlating with an intermediate tonicity between phasic bladder and tonic aorta with a rapid increase in force development but also with extended force maintenance at the functional level. Meanwhile, isoforms of NMMHC-A, B, C were also abundantly detected in rat prostate with SMM present only in SM, NMMHC-A, B, C isoforms both present in stromal and endothelial cells in rat prostate. But in human prostatic cell lines, NMMHC-C expressed only in the SM cells, which was different to rat prostate. At the functional level, the SMM selective inhibitor BLEB could potently relax rat prostate SM, comparable to SNP and H-1152.

The prostatic SM represents a significant component of the stroma. In the present study, it was identified using the highly specific SM marker MHC and its spatial arrangement in the stroma was uncovered. It is assumed this arrangement is not optimal for force generation. However, we observed that it did produce significant force in response to either KCl or PE (Figs 3A and 4A). Thus, the active forces in the prostatic tissue might play an important role in the pathophysiology of BPH. However, until now the contractile properties of prostatic SM have not been well characterized. Lin *et al.* [53] characterized the expression of SM MHC and NM MHC at both peptide and mRNA levels in human prostate tissue and only demonstrated that both SM1 and SM2 isoforms are expressed in prostate but not in fibroblast cells. In current study, we thoroughly characterized rat prostate SM isoforms and found it expressed almost equal SM-B (58.8%), mainly LC_{17a} (83.8%) and less SM2 (11.4%). When compared to rat CC SM which expressed SM-B (70.4%), almost equal LC_{17a} (48.7%) and less SM2 (28.9%), a difference was demonstrated between prostate and CC. Thus, there may be organ level differences in SM myosin isoform composition among these different tissues. However, at the functional level, both prostate and CC SM displayed an intermediate contraction phenotype between phasic bladder and tonic aorta (Fig. 4).

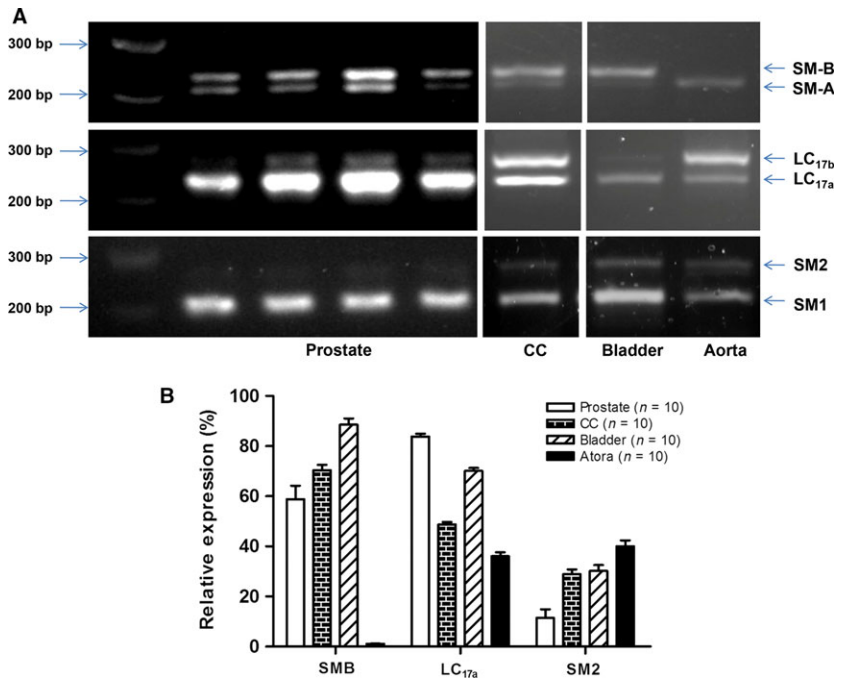

Fig. 5 (**A**) RT-PCR bands of smooth muscle myosin (SMM) isoforms in rat ventral prostate, corpus cavernosum (CC), bladder and aorta. Representative GelStar-stained agarose gels of cDNA products resulting from competitive RT-PCR analysis were utilized to detect the expression of SM-A/SM-B, LC_{17a}/LC_{17b} and SM1/SM2 isoforms. Four lanes in the panel 'prostate' represent four different prostate samples. (**B**) The summary graph for the expression of SMM isoforms in rat ventral prostate, CC, bladder and aorta. Averaged quantitative determination of SMM pre-mRNA mean isoform percentages in ventral prostate, CC, bladder and aorta was determined by reflectance scanning of gel photographs, and subsequent analyses were conducted by the Bio-Rad Molecular Analyst 1D program. Values are expressed as mean ± S.E.M. (n = 10 different animals for each group).

Table 2 Time to 50% phenylephrine (PE) or carbachol-mediated maximum contraction for prostate, corpus cavernosum (CC), bladder and aorta

Tissue	Number	Time (sec.)	*P* value (compared to Prostate)
Prostate	10	13.2 ± 2.6	NS
CC	8	12.7 ± 2.5	NS
Bladder	10	5.2 ± 1.2	<0.01
Aorta	7	24.2 ± 2.4	<0.01

CC: corpus cavernosum; NS: no significance; PE: phenylephrine.

Previous studies demonstrated the SM-B isoform was associated with SM tissues with a more phasic contractile nature, faster shortening velocity and higher ATPase activity, whereas the SM-A isoform was found in a slower and more tonic type SM with lower ATPase activity [17–20]. Similarly, the relative higher ratio of the LC_{17a} to LC_{17b} isoform was also demonstrated a more phasic contraction [18, 54, 55]. Indeed, the present study showed that rat aorta expressed exclusively SM-A and less LC_{17a} favouring a slow tonic contraction (Fig. 4D), while rat bladder expressed almost exclusively SM-B and predominantly LC_{17a} exhibiting a fast phasic contraction (Fig. 4C). Consistent with these observations, the time to 50% maximum contraction was 24.2 sec. for aorta, which was 4-fold longer than that for bladder. Also consistent was the demonstration that the rat prostate expressed almost equal SM-B relative to SM-A correlating with an intermediate contraction phenotype and time to 50% maximum contraction between bladder and aorta (Table 2), although over 80% LC_{17a} was detected. It was reported the effect of LC_{17} isoforms in shortening velocity might be confounded by differences in SM-A/B isoforms. Interestingly, Rovner *et al.* [56] reported an approximate 2-fold higher *in vitro* motility speed and Mg^{2+}-ATPase activity in expressed SM-B heavy meromyosin regardless of the LC_{17} isoforms present (pure LC_{17a} or pure LC_{17b}). Further supporting the Rovner *et al.* observation, Sweeney *et al.* [57] reported that *in vitro* motility sliding velocity and actin-ATPase activity correlated with increasing loop size/flexibility but were not affected by the LC_{17} isoforms present. X-ray crystallography data have revealed that the LC_{17} subunits can approach the 25/50-kD loop, which is the location of the NH2-terminal SM-A-/B isoforms and near the nucleotide binding pocket of myosin and regulates the opening for the nucleotide binding cleft [54, 57]. Although it is unclear whether this is a physiologically relevant observation, it is intriguing because a possible interaction between

Journal of Cellular and Molecular Medicine published by John Wiley & Sons Ltd and Foundation for Cellular and Molecular Medicine.

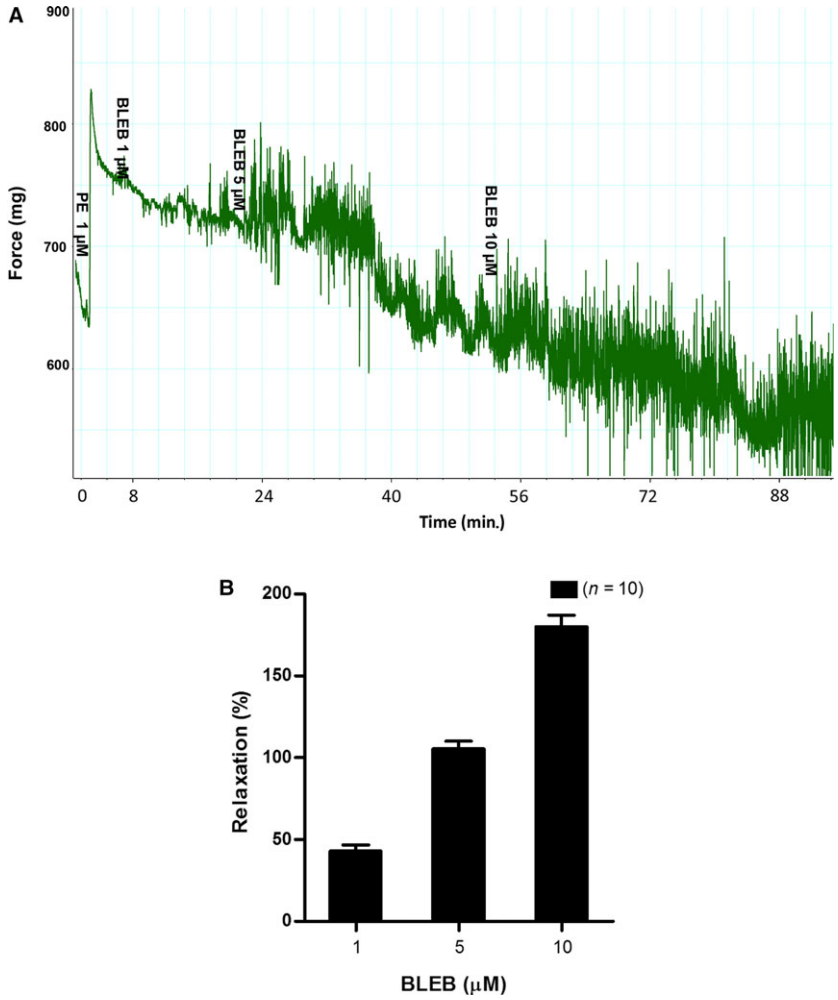

Fig. 6 (**A**) The representative tracings of BLEB-induced relaxation effects on ventral prostate pre-contracted with PE. Ventral prostate strips pre-contracted with 1 μM PE were allowed to reach stable tension, and then, the relaxant effect of increasing doses of BLEB (1, 5, 10 μM) was evaluated. The *x*-axis represents time (min.), while the *y*-axis represents force (mg). (**B**) Summary graph of BLEB-induced relaxation effects on ventral prostate. Response to stimulus was taken as 100%, while the relaxation or inhibitory effect of BLEB was evaluated as a percentage of this response. Values are expressed as mean ± S.E.M. (*n* = strips obtained from 10 different animals).

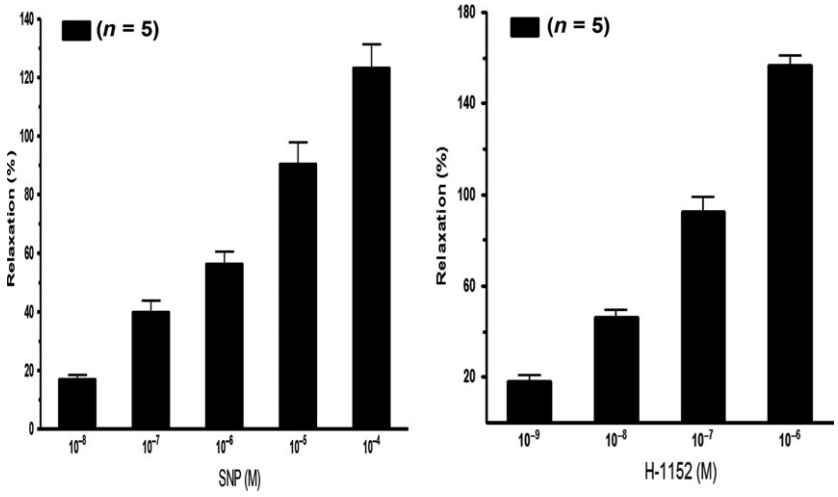

Fig. 7 Summary graphs of nitric oxide (NO) donor sodium nitroprusside (SNP) and Rho-kinase inhibitor H-1152 on rat prostate pre-contracted with phenylephrine (PE). The left panel and right panel display summary graphs of SNP and H-1152 relaxation effects on PE-pre-contracted rat ventral prostate strips, respectively. Response to stimulus was taken as 100%, while the relaxation effects of SNP and H-1152 were evaluated as a percentage of this response. Values are expressed as mean ± S.E.M. (*n* = strips obtained from five different animals).

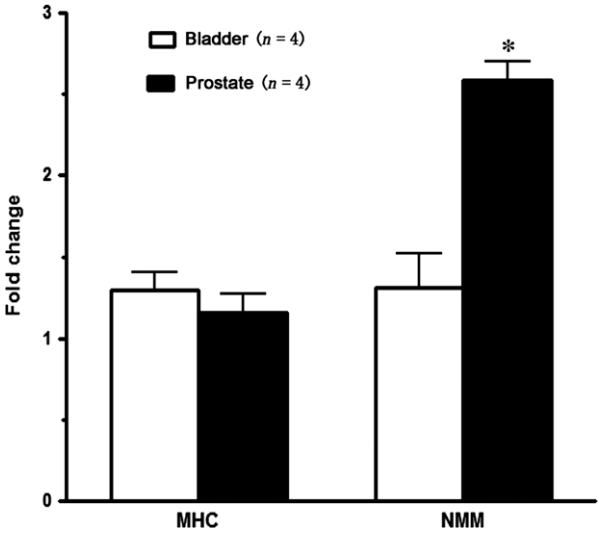

Fig. 8 Expression of total smooth muscle myosin heavy chain (SM MHC) and non-muscle myosin heavy chain B (NMMHC-B) in rat ventral prostate and bladder. Total SM MHC and NMMHC-B were quantified by real-time RT-PCR. Expression is normalized to the RPL19 housekeeping gene. Values are expressed as mean ± S.E.M. * equals $P < 0.05$ ($n = 4$ different animals for each group).

the variable sizes of SM-A/B isoforms and $LC_{17a/b}$ isoforms could help resolve the apparent discrepancy in the data for a possible role of the LC_{17} isoforms in the regulation of unloaded shortening velocity in SM tissues. The SM MHC tail isoforms (SM1 and SM2) in rat prostate, CC, bladder and aorta showed differences in levels of expression, but there seemed to be no obvious correlation with muscle shortening velocity in our study. Sparrow *et al.* [58] also concluded that there are no obvious differences in the intrinsic properties of these two isoforms. They found a small positive correlation between SM1 expression and unloaded shortening in skinned rat myometrial muscle, but a small inverse correlation was confirmed in intact tissue. This discrepancy might be due to inherent differences in these two model systems.

In contrast to the role of SMM in mediating contraction, NMM had been proposed to be involved in cellular 'housekeeping'-type processes, including proliferative, synthetic and secretory functions [27, 59, 60]. In the present study, we found that NMMHC-A, B and C were present both in SM and endothelial cells of rat prostate, and NMMHC-A and NMMHC-B were present in HPrSMCs as well as HprECs, However, NMMHC-C was expressed only in the HPrSMCs. Golomb *et al.* also found that NMMHC-C is expressed in the apical area of epithelial cells in the inner ear of mouse. Thus the different location of NMMHC-C in SM or endothelial cells might attributable to the different tissue from different species. As NMMHC-A had the highest rate

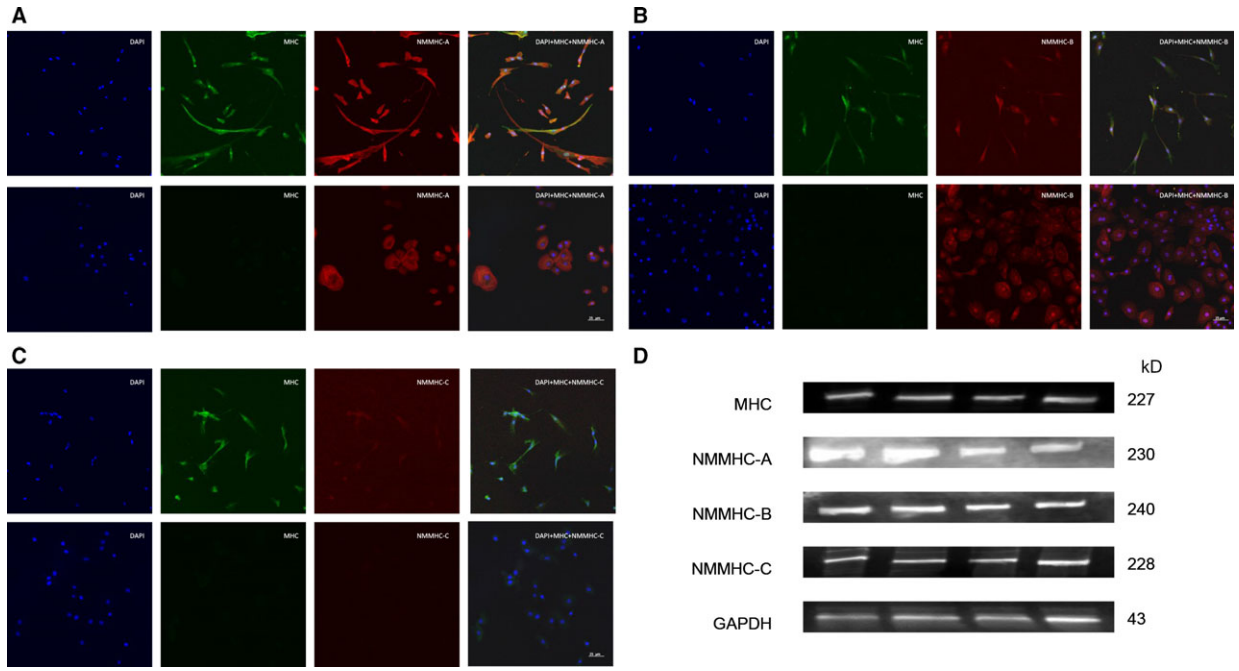

Fig. 9 Immunolocalization of SM MHC and NM MHC isoforms in HPrSMCs and HPrECs and expression of SM MHC and NM MHC isoforms in rat prostate. HPrSMCs (upper subpanels of **A**, **B** and **C**) and HPrECs (lower subpanels of **A**, **B** and **C**) were processed as described in the Materials and methods. Double immunofluorescence staining for NMM isoforms (NMMHC-A, NMMHC-B and NMMHC-C) (red fluorescence) and SM MHC (green fluorescence) was conducted in HPrSMCs and HPrECs. Nuclei were stained by DAPI (blue). The images were photographed by confocal fluorescence microscopy. The scale bars for (**A**)–(**C**) are 25 μm. (**D**) Representative Western blotting bands (from top to bottom) of SM MHC and NMM isoforms (NMMHC-A, NMMHC-B and NMMHC-C) and GAPDH in rat ventral prostate.

Journal of Cellular and Molecular Medicine published by John Wiley & Sons Ltd and Foundation for Cellular and Molecular Medicine.

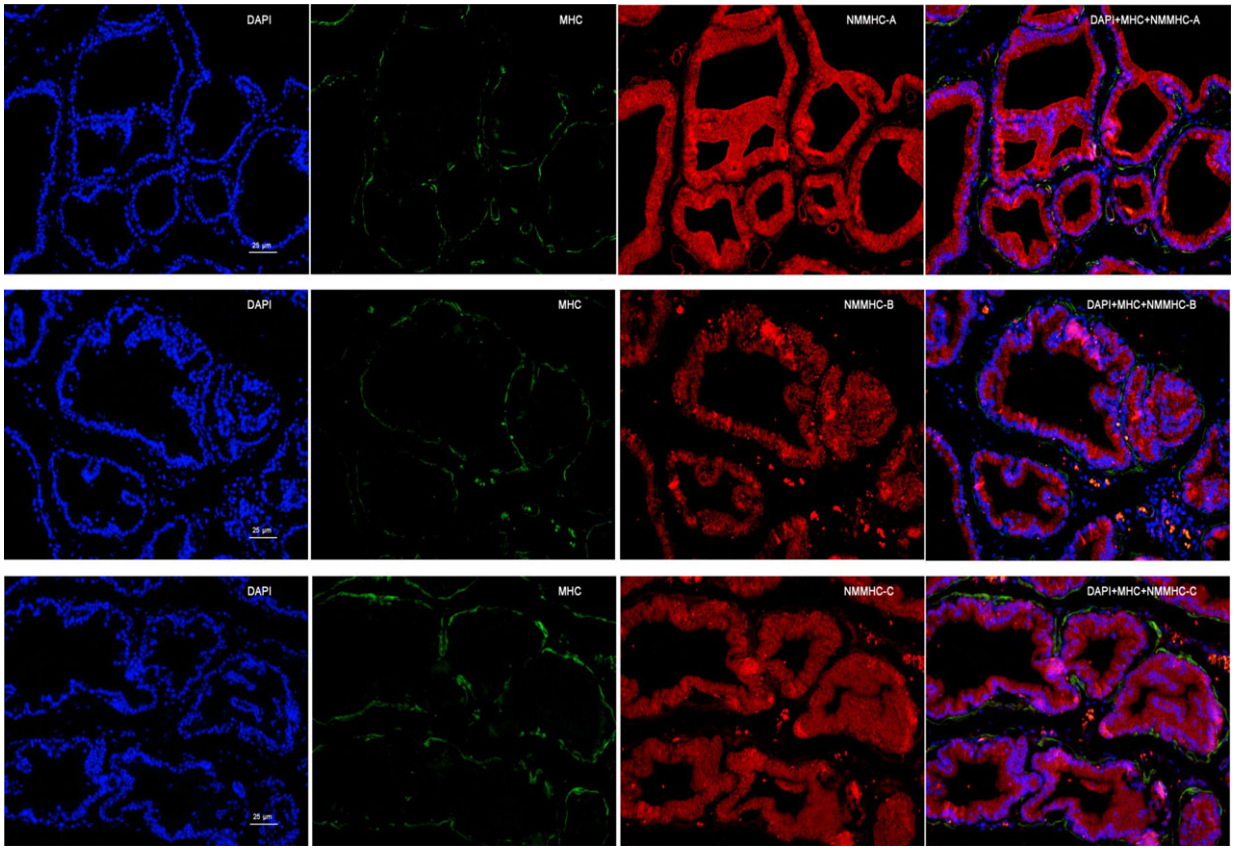

Fig. 10 Immunolocalization of SM MHC and NM MHC isoforms in rat prostate. Representative double immunofluorescence staining for NMMHC-A (top), NMMHC-B (middle) and NMMHC-C (bottom) (red fluorescence) and SM MHC (green fluorescence) was conducted in rat prostate. Nuclei were stained by DAPI (blue). The images were photographed by confocal fluorescence microscopy. The scale bars represent 25 μm.

of ATP hydrolysis of the three NMM isoforms [28] and NMMHC-B played an ancillary role in SM contraction, they might have distinct functions in the maintenance of tension during tonic contractions [29, 30]. In our current study, we found NMMHC-B expressed more than 2-fold higher in rat prostate than in rat bladder. It was further suggested that NMM might also play an important role in cell proliferation and BPH development. Interestingly, NMMHC-C is the newest identified NMM isoform with presently unknown roles. Therefore, it seems to be clearly worth determining the functional activity of these NMM isoforms in the prostate in the future.

Finally, we showed PE pre-contracted prostate SM can be potently relaxed by BLEB (a selective myosin inhibitor), comparable to the effect of SNP (NO donor) and H-1152 (a specific, strong and membrane-permeable inhibitor of Rho-kinase). Although BLEB was originally reported to be a selective inhibitor of the myosin II isoforms expressed by striated muscles and non-muscle (IC_{50} = 0.5–5 μM) but a poor inhibitor of purified turkey smooth muscle myosin II (IC_{50} ~80 μM) [46], our previous studies have clearly demonstrated that BLEB is indeed also a potent inhibitor for rat bladder and CC SM [44, 45]. In current study, we found that BLEB is a potent inhibitor for rat prostate SM and can significantly relax prostate SM at a concentration of 3 μM, comparable with the range of IC_{50} values (~3–5 μM) for SM of chicken arteries reported by Eddinger *et al.* Interesting to note is that Eddinger *et al.* [43] also found that contraction of chicken gizzard was less potently inhibited by BLEB. Thus, an additional protein was assumed to uniquely exist in avian gizzard and reduced the effectiveness of BLEB. As it has been suggested that BLEB efficacy may be impacted by the relative expression of the SM-A/B isoforms composition [37], the more relatively expressed SM-B in the prostate could contribute to the potent relaxing effect of BLEB for this kind of SM. In addition, BLEB was originally discovered as a selective inhibitor of NMM [16] and the abundant expression of NMMHC-A and B isoforms in the prostate SM found in current study could also contribute to the strong inhibitory ability of BLEB in this tissue. As NMM plays an important role in cell proliferation, it is plausible that inhibiting or knocking down NMM could prevent prostate growth. Indeed, we found atrophy of prostate when BLEB was injected into rat prostate *in vivo* (data not shown). Therefore, prostate SMM or NMM could be a promising target for discovering new drugs for treating BPH.

A limitation for the current study is that the protein levels of SMM isoforms were not determined as isoform-specific antibodies are not commercial available at present. However, a previous study

demonstrated that mRNA levels of SMM isoforms correlated well with protein expression [61]. Another weakness is that the functional activities of SMM and NMM isoforms cannot be distinguished in the prostate, although their isoforms composition was accurately determine.

In conclusion, we demonstrated, for the first time, the expression, characterization, composition and functional activities of SMM and NMM isoforms in the rat prostate. It is suggested that the isoforms of SMM and NMM could play important roles in the development and clinical effects of BPH.

Acknowledgements

P.C., X.H.Z., J.Y., X.H.W. and M.E.D. designed the experiment and P.C. wrote the first draft. P.C. and J.Y. conducted most of the experiments, Y.M.G. and H.X. helped to analyse the results. X.H.Z. and M.E.D. critically revised drafts of the manuscript, provided important intellectual input and approved the final version for publication.

Funding source

X.H.Z. is supported by National Natural Science Foundation of China (Nos. 81270843 and 81160086).

Conflict of interest

The authors declare that they have no competing interests.

References

1. **Bushman W.** Etiology, epidemiology, and natural history of benign prostatic hyperplasia. *Urol Clin North Am*. 2009; 36: 403–15, v.
2. **Roehrborn CG.** Benign prostatic hyperplasia: an overview. *Rev Urol*. 2005; 7(Suppl. 9): S3–14.
3. **McConnell JD.** Medical management of benign prostatic hyperplasia with androgen suppression. *Prostate Suppl*. 1990; 3: 49–59.
4. **Caine M.** Alpha-adrenergic mechanisms in dynamics of benign prostatic hypertrophy. *Urology*. 1988; 32: 16–20.
5. **O'Leary MP, Roehrborn CG, Black L.** Dutasteride significantly improves quality of life measures in patients with enlarged prostate. *Prostate Cancer Prostatic Dis*. 2008; 11: 129–33.
6. **Shapiro E, Becich MJ, Hartanto V, *et al.*** The relative proportion of stromal and epithelial hyperplasia is related to the development of symptomatic benign prostate hyperplasia. *J Urol*. 1992; 147: 1293–7.
7. **Zhang X, Zang N, Wei Y, *et al.*** Testosterone regulates smooth muscle contractile pathways in the rat prostate: emphasis on PDE5 signaling. *Am J Physiol Endocrinol Metab*. 2012; 302: E243–53.
8. **Gu H, Martin H, Barsotti RJ, *et al.*** Rapid increase in inositol phosphate levels in norepinephrine-stimulated vascular smooth muscle. *Am J Physiol*. 1991; 261: C17–22.
9. **Sward K, Mita M, Wilson DP, *et al.*** The role of RhoA and Rho-associated kinase in vascular smooth muscle contraction. *Curr Hypertens Rep*. 2003; 5: 66–72.
10. **Adelstein RS, Eisenberg E.** Regulation and kinetics of the actin-myosin-ATP interaction. *Annu Rev Biochem*. 1980; 49: 921–56.
11. **Babij P, Kelly C, Periasamy M.** Characterization of a mammalian smooth muscle myosin heavy-chain gene: complete nucleotide and protein coding sequence and analysis of the 5′ end of the gene. *Proc Natl Acad Sci USA*. 1991; 88: 10676–80.
12. **Babij P, Periasamy M.** Myosin heavy chain isoform diversity in smooth muscle is produced by differential RNA processing. *J Mol Biol*. 1989; 210: 673–9.
13. **Lenz S, Lohse P, Seidel U, *et al.*** The alkali light chains of human smooth and nonmuscle myosins are encoded by a single gene. Tissue-specific expression by alternative splicing pathways. *J Biol Chem*. 1989; 264: 9009–15.
14. **Nabeshima Y, Nabeshima Y, Nonomura Y, *et al.*** Nonmuscle and smooth muscle myosin light chain mRNAs are generated from a single gene by the tissue-specific alternative RNA splicing. *J Biol Chem*. 1987; 262: 10608–12.
15. **Babu GJ, Loukianov E, Loukianova T, *et al.*** Loss of SM-B myosin affects muscle shortening velocity and maximal force development. *Nat Cell Biol*. 2001; 3: 1025–9.
16. **Straight AF, Cheung A, Limouze J, *et al.*** Dissecting temporal and spatial control of cytokinesis with a myosin II Inhibitor. *Science*. 2003; 299: 1743–7.
17. **DiSanto ME, Cox RH, Wang Z, *et al.*** NH2-terminal-inserted myosin II heavy chain is expressed in smooth muscle of small muscular arteries. *Am J Physiol*. 1997; 272: C1532–42.
18. **DiSanto ME, Wang Z, Menon C, *et al.*** Expression of myosin isoforms in smooth muscle cells in the corpus cavernosum penis. *Am J Physiol*. 1998; 275: C976–87.
19. **Hypolite JA, DiSanto ME, Zheng Y, *et al.*** Regional variation in myosin isoforms and phosphorylation at the resting tone in urinary bladder smooth muscle. *Am J Physiol Cell Physiol*. 2001; 280: C254–64.
20. **Kelley CA, Takahashi M, Yu JH, *et al.*** An insert of seven amino acids confers functional differences between smooth muscle myosins from the intestines and vasculature. *J Biol Chem*. 1993; 268: 12848–54.
21. **Koi PT, Milhoua PM, Monrose V, *et al.*** Expression of myosin isoforms in the smooth muscle of human corpus cavernosum. *Int J Impot Res*. 2007; 19: 62–8.
22. **Vignozzi L, Filippi S, Morelli A, *et al.*** Effect of chronic tadalafil administration on penile hypoxia induced by cavernous neurotomy in the rat. *J Sex Med*. 2006; 3: 419–31.
23. **Katsuragawa Y, Yanagisawa M, Inoue A, *et al.*** Two distinct nonmuscle myosin-heavy-chain mRNAs are differentially expressed in various chicken tissues. Identification of a novel gene family of vertebrate non-sarcomeric myosin heavy chains. *Eur J Biochem FEBS*. 1989; 184: 611–6.
24. **Shohet RV, Conti MA, Kawamoto S, *et al.*** Cloning of the cDNA encoding the myosin heavy chain of a vertebrate cellular myosin. *Proc Natl Acad Sci USA*. 1989; 86: 7726–30.
25. **Simons M, Wang M, McBride OW, *et al.*** Human nonmuscle myosin heavy chains are encoded by two genes located on different chromosomes. *Circ Res*. 1991; 69: 530–9.
26. **Golomb E, Ma X, Jana SS, *et al.*** Identification and characterization of nonmuscle myosin II-C, a new member of the myosin II family. *J Biol Chem*. 2004; 279: 2800–8.
27. **Eddinger TJ, Meer DP.** Myosin II isoforms in smooth muscle: heterogeneity and

Journal of Cellular and Molecular Medicine published by John Wiley & Sons Ltd and Foundation for Cellular and Molecular Medicine.

function. *Am J Physiol Cell Physiol*. 2007; 293: C493–508.

28. **Swailes NT, Colegrave M, Knight PJ, *et al.*** Non-muscle myosins 2A and 2B drive changes in cell morphology that occur as myoblasts align and fuse. *J Cell Sci*. 2006; 119: 3561–70.
29. **Yuen SL, Ogut O, Brozovich FV.** Nonmuscle myosin is regulated during smooth muscle contraction. *Am J Physiol Heart Circ Physiol*. 2009; 297: H191–9.
30. **Morano I, Chai GX, Baltas LG, *et al.*** Smooth-muscle contraction without smooth-muscle myosin. *Nat Cell Biol*. 2000; 2: 371–5.
31. **Vicente-Manzanares M, Choi CK, Horwitz AR.** Integrins in cell migration–the actin connection. *J Cell Sci*. 2009; 122: 199–206.
32. **Ballestrem C, Erez N, Kirchner J, *et al.*** Molecular mapping of tyrosine-phosphorylated proteins in focal adhesions using fluorescence resonance energy transfer. *J Cell Sci*. 2006; 119: 866–75.
33. **Ponti A, Machacek M, Gupton SL, *et al.*** Two distinct actin networks drive the protrusion of migrating cells. *Science*. 2004; 305: 1782–6.
34. **Jay PY, Pham PA, Wong SA, *et al.*** A mechanical function of myosin II in cell motility. *J Cell Sci*. 1995; 108: 387–93.
35. **Arafat HA, Kim GS, DiSanto ME, *et al.*** Heterogeneity of bladder myocytes *in vitro*: modulation of myosin isoform expression. *Tissue Cell*. 2001; 33: 219–32.
36. **Eddinger TJ, Murphy RA.** Developmental changes in actin and myosin heavy chain isoform expression in smooth muscle. *Arch Biochem Biophys*. 1991; 284: 232–7.
37. **Zhang X, Seftel A, DiSanto ME.** Blebbistain, a myosin II inhibitor, as a novel strategy to regulate detrusor contractility in a rat model of partial bladder outlet obstruction. *PLoS ONE*. 2011; 6: e25958.
38. **Cunha GR, Chung LW, Shannon JM, *et al.*** Stromal-epithelial interactions in sex differentiation. *Biol Reprod*. 1980; 22: 19–42.
39. **Cunha GR, Chung LW, Shannon JM, *et al.*** Hormone-induced morphogenesis and growth: role of mesenchymal-epithelial interactions. *Recent Prog Horm Res*. 1983; 39: 559–98.
40. **Cunha GR, Hayward SW, Wang YZ, *et al.*** Role of the stromal microenvironment in carcinogenesis of the prostate. *Int J Cancer*. 2003; 107: 1–10.
41. **Cunha GR, Donjacour A.** Stromal-epithelial interactions in normal and abnormal prostatic development. *Prog Clin Biol Res*. 1987; 239: 251–72.
42. **Cunha GR.** Role of mesenchymal-epithelial interactions in normal and abnormal development of the mammary gland and prostate. *Cancer*. 1994; 74: 1030–44.
43. **Eddinger TJ, Meer DP, Miner AS, *et al.*** Potent inhibition of arterial smooth muscle tonic contractions by the selective myosin II inhibitor, blebbistatin. *J Pharmacol Exp Ther*. 2007; 320: 865–70.
44. **Zhang X, Kuppam DS, Melman A, *et al.*** *In vitro* and *in vivo* relaxation of urinary bladder smooth muscle by the selective myosin II inhibitor, blebbistatin. *BJU Int*. 2011; 107: 310–7.
45. **Zhang XH, Aydin M, Kuppam D, *et al.*** *In vitro* and *in vivo* relaxation of corpus cavernosum smooth muscle by the selective myosin II inhibitor, blebbistatin. *J Sex Med*. 2009; 6: 2661–71.
46. **Limouze J, Straight AF, Mitchison T, *et al.*** Specificity of blebbistatin, an inhibitor of myosin II. *J Muscle Res Cell Motil*. 2004; 25: 337–41.
47. **Zhang XH, Morelli A, Luconi M, *et al.*** Testosterone regulates PDE5 expression and *in vivo* responsiveness to tadalafil in rat corpus cavernosum. *Eur Urol*. 2005; 47: 409–16; discussion 16.
48. **Granchi S, Vannelli GB, Vignozzi L, *et al.*** Expression and regulation of endothelin-1 and its receptors in human penile smooth muscle cells. *Mol Hum Reprod*. 2002; 8: 1053–64.
49. **Yamamoto M, Harm SC, Grasser WA, *et al.*** Parathyroid hormone-related protein in the rat urinary bladder: a smooth muscle relaxant produced locally in response to mechanical stretch. *Proc Natl Acad Sci USA*. 1992; 89: 5326–30.
50. **Ghasemi M, Sadeghipour H, Shafaroodi H, *et al.*** Role of the nitric oxide pathway and the endocannabinoid system in neurogenic relaxation of corpus cavernosum from biliary cirrhotic rats. *Br J Pharmacol*. 2007; 151: 591–601.
51. **Ren J, Wang GJ, Petrovski P, *et al.*** Influence of hypertension on acetaldehyde-induced vasorelaxation in rat thoracic aorta. *Pharmacol Res*. 2002; 45: 195–9.
52. **Livak KJ, Schmittgen TD.** Analysis of relative gene expression data using real-time quantitative PCR and the 2(−Delta Delta C(T)) Method. *Methods*. 2001; 25: 402–8.
53. **Lin VK, Wang D, Lee IL, *et al.*** Myosin heavy chain gene expression in normal and hyperplastic human prostate tissue. *Prostate*. 2000; 44: 193–203.
54. **Dominguez R, Freyzon Y, Trybus KM, *et al.*** Crystal structure of a vertebrate smooth muscle myosin motor domain and its complex with the essential light chain: visualization of the pre-power stroke state. *Cell*. 1998; 94: 559–71.
55. **Malmqvist U, Arner A.** Correlation between isoform composition of the 17 kDa myosin light chain and maximal shortening velocity in smooth muscle. *Pflugers Archiv*. 1991; 418: 523–30.
56. **Rovner AS, Freyzon Y, Trybus KM.** An insert in the motor domain determines the functional properties of expressed smooth muscle myosin isoforms. *J Muscle Res Cell Motil*. 1997; 18: 103–10.
57. **Sweeney HL, Rosenfeld SS, Brown F, *et al.*** Kinetic tuning of myosin *via* a flexible loop adjacent to the nucleotide binding pocket. *J Biol Chem*. 1998; 273: 6262–70.
58. **Sparrow MP, Mohammad MA, Arner A, *et al.*** Myosin composition and functional properties of smooth muscle from the uterus of pregnant and non-pregnant rats. *Pflugers Archiv*. 1988; 412: 624–33.
59. **Obara K, Bilim V, Suzuki K, *et al.*** Transforming growth factor-beta1 regulates cell growth and causes downregulation of SMemb/non-muscle myosin heavy chain B mRNA in human prostate stromal cells. *Scand J Urol Nephrol*. 2005; 39: 366–71.
60. **Hindman B, Goeckeler Z, Sierros K, *et al.*** Non-muscle myosin II isoforms have different functions in matrix rearrangement by MDA-MB-231 Cells. *PLoS ONE*. 2015; 10: e0131920.
61. **DiSanto ME, Stein R, Chang S, *et al.*** Alteration in expression of myosin isoforms in detrusor smooth muscle following bladder outlet obstruction. *Am J Physiol Cell Physiol*. 2003; 285: C1397–410.